ECOGRAPHY

Research

The role of habitat fragmentation in Pleistocene megafauna extinction in Eurasia

Alessandro Mondanaro*, Mirko Di Febbraro*, Marina Melchionna, Luigi Maiorano, Moreno Di Marco, Neil R. Edwards, Philip B. Holden, Silvia Castiglione, Lorenzo Rook and Pasquale Raia

A. Mondanaro (https://orcid.org/0000-0003-0325-7066) and L. Rook, Dept of Earth Science, Univ. of Florence, Florence, Italy. – AM, M. Melchionna, S. Castiglione and P. Raia (https://orcid.org/0000-0002-4593-8006) ✉ (pasquale.raia@unina.it), Dept of Earth, Environmental and Resources Sciences, Univ. of Naples 'Federico II', Naples, Italy. – M. Di Febbraro (https://orcid.org/0000-0001-8898-7046), Dept of Bioscience and Territory, Univ. of Molise, Pesche, Isernia, Italy. – L. Maiorano (https://orcid.org/0000-0002-2957-8979) and M. Di Marco, Dept of Biology and Biotechnologies 'Charles Darwin', Univ. of Rome 'La Sapienza', Roma, Italy. – N. R. Edwards (https://orcid.org/0000-0001-6045-8804) and P. B. Holden, School of Environment, Earth and Ecosystem Sciences, The Open Univ., Milton Keynes, UK.

Ecography
44: 1619–1630, 2021
doi: 10.1111/ecog.05939

Subject Editor: Kate Lyons
Editor-in-Chief: Miguel Araújo
Accepted 2 August 2021

The idea that several small, rather than a single large, habitat areas should hold the highest total species richness (the so-called SLOSS debate) brings into question the importance of habitat fragmentation to extinction risk. SLOSS studies are generally addressed over a short time scale, potentially ignoring the long-term dimension of extinction risk. Here, we provide the first long-term evaluation of the role of habitat fragmentation in species extinction, focusing on 22 large mammal species that lived in Eurasia during the last 200 000 years. By combining species distribution models and landscape pattern analysis, we compared temporal dynamics of habitat spatial structure between extinct and extant species, estimating the size, number and degree of the geographical isolation of their suitable habitat patches. Our results evidenced that extinct mammals went through considerable habitat fragmentation during the last glacial period and started to fare worse than extant species from about 50 ka. In particular, our modelling effort constrains the fragmentation of habitats into a narrow time window, from 46 to 36 ka ago, surprisingly coinciding with known extinction dates of several megafauna species. Landscape spatial structure was the second most important driver affecting megafauna extinction risk (ca 38% importance), after body mass (ca 39%) and followed by dietary preferences (ca 20%). Our results indicate a major role played by landscape fragmentation on extinction. Such evidence provides insights on what might likely happen in the future, with climate change, habitat loss and fragmentation acting as the main forces exerting their negative effects on biodiversity.

Keywords: habitat fragmentation, landscape metrics, linear mixed models, megafauna, species distribution models, species extinction

Introduction

Humans control most of Earth's net primary productivity (Liu et al. 2019, Ripple et al. 2019, Williams et al. 2020) and are stressing natural habitats to an unprecedented

*Equally contributed.

NORDIC SOCIETY OIKOS

www.ecography.org

degree, raising extinction rates to the level of mass extinction (Ceballos et al. 2015, Andermann et al. 2020). Human pressure also exerts a negative impact on ecosystem functioning, depressing ecosystems' resilience and therefore the chance for species to recover when (and if) human pressure is relieved (Lyons et al. 2016, Pimiento et al. 2020). The pervasive presence of humans is impacting the extension and diversity of natural habitats as well, leaving wildlife with little space to survive (Newbold et al. 2015). In this context, it becomes necessary to understand how habitat availability and fragmentation will affect the chance of species survival in the long term.

Diamond (1975) first proposed on theoretical grounds that a single large undisturbed habitat should hold more species than several small habitat patches amounting to the same total area. This idea attracted enormous interest, generating the so-called SLOSS (single large or several small) debate (Tjørve 2010). Although elegant and intuitive, Diamond's conjecture received little empirical support, with most studies pointing to the opposite effect, that is many small patches generally hold more species than a single patch of the same overall extent (Fahrig et al. 2019). Fahrig (2013) proposed that species richness in a given place increases with the amount of habitat present in the surrounding area, whereas the size and isolation of individual habitat patches within the area are unimportant. This 'habitat amount hypothesis' (HAH), then implies that the degree of fragmentation, as well as any other habitat geographic configuration characteristics, does not affect the chance of species survival. The HAH was recently tested in several studies (Fahrig 2020), pushing the balance towards the several small sides of the SLOSS debate. Apparently, this result holds true for specialist and threatened species, suggesting that it is not simply arising from incursion by generalist species into small patches, as often suggested. Moreover, the result does not change when considering natural or anthropogenic landscapes (Fahrig 2020). Yet, Saura (2021) questioned Fahrig's findings on methodological grounds, proposing evidence for a strong influence of habitat spatial structure (i.e. the spatial arrangement of suitable habitat patches) on HAH predictions. Saura (2021) noted that habitat fragmentation, while holding the amount of habitat constant, negatively affects species richness. The HAH debate is intriguing, both because it has no clear-cut explanation and because it contrasts with the several studies demonstrating large and well-connected habitat patches are beneficial to species' survival (Fahrig 2003, Reed 2004, Blomqvist et al. 2010, Haddad et al. 2015, Lino et al. 2019).

One major limitation of SLOSS studies is that they fail to capture the potential long-term effects of habitat fragmentation on species persistence by focusing on living wildlife and on a short temporal scale (Fahrig 2020). This suggests that even if HAH holds true, it does not preclude a detrimental effect of habitat fragmentation on species survival in the long run. Here, we provide the first long-term analysis of the importance of habitat fragmentation (as defined by patch size, number and degree of isolation) to species extinction, using the dense fossil record of Late Pleistocene large mammals of Eurasia and fine resolution paleoclimatic data. We apply species distribution modelling and landscape metrics (i.e. metrics quantifying the amount and the spatial arrangement of habitable patches) to 31 different large mammal species that lived in Eurasia during the last 200 000 years (200 ka). We compare landscape metrics for extinct and extant species, to estimate the difference in size, number and geographical isolation of habitat patches and their influence on extinction risk.

Material and methods

Mammal database

We collected fossil occurrences for 21 extinct and 10 extant large mammals living in Eurasia during the last 200 ka, belonging to the orders of Artiodactyla, Carnivora, Perissodactyla and Proboscidea. We enriched the fossil mammal occurrence databases published in Raia et al. (2009) and Carotenuto et al. (2016), by adding new records and supplementing stratigraphic context and aging of the fossil layers. Radiocarbon dates were calibrated by using the 'Bchron' R package (Parnell 2016), applying the 'Intcal20' calibration curve (Reimer et al. 2020). Overall, we obtained 4651 mammal occurrences distributed over 916 geological or fossil layers (Supporting information). For each species considered, we collected data on body mass and prevalent diet from Lundgren et al. (2021). We considered three categories of diet: grasses, browse and vertebrate meat. For each category, we expressed diet as a rank from 0 to 3 indicating an increasing degree of specialization in the consumption of each category.

Climatic predictors

Climate variables were generated using a paleoclimate emulator, following the methodology of Holden et al. (2019). The approach applies Gaussian process emulation of the singular value decomposition of ensembles of runs from the intermediate complexity atmosphere-ocean model PLASIM-GENIE (Holden et al. 2016) with varied boundary-condition forcing. Spatial fields of monthly temperature and precipitation were emulated at 1000-year intervals, driven by time-series of scalar boundary-condition forcing of CO_2 (Lüthi et al. 2008), orbit (Berger and Loutre 1999) and ice-volume (Stap et al. 2017), and assuming the climate is in quasi-equilibrium. Monthly emulated paleoclimate bioclimatic variables at resolution 5° were transformed into anomalies and downscaled onto modern observations (CHELSA; Karger et al. 2017) at 0.5° spatial resolution using bilinear interpolation.

Seventeen of the nineteen bioclimatic variables (Karger et al. 2017) were generated, omitting annual mean diurnal range (BIO2) and isothermality (BIO3) because the diurnal cycle was not simulated. Monthly mean temperature anomalies were applied for the maximum temperature of the warmest month (BIO5) and the minimum temperature of

the coldest month (BIO6), assuming that temporal variability within each month is constant through time. Temperature anomalies were combined with the modern baselines additively. Precipitation anomalies were combined with baselines using a mixed multiplicative/additive approach (Holden et al. 2019). Variables were then projected under a Mollweide coordinate reference system and a 50 × 50 km spatial resolution. To avoid potential problems of multicollinearity, the full set of 17 bioclimatic variables was sub-selected considering a variance inflation factor ≤ 5 (Zuur et al. 2010) through the 'usdm' R package (Naimi et al. 2014), retaining the following seven predictors: BIO4 (temperature seasonality), BIO5 (maximum temperature of the warmest month), BIO8 (mean temperature of the wettest quarter), BIO13 (precipitation of wettest month), BIO14 (precipitation of driest month), BIO18 (precipitation of warmest quarter) and precipitation of coldest quarter (BIO19).

Species distribution models (SDMs)

Age estimates for fossil layers come with some uncertainty. To account for this, following Raia et al. (2020), we generated a set of 100 SDM replications for each species. At each replication, for each fossil site, the age was drawn from a uniform distribution ranging from the minimum to the maximum age estimate of the site. For each species, any single replicate included all the species presences plus 10 000 pseudoabsences (Supporting information). The latter was generated by randomly placing 10 000 background points within a minimum convex polygon enclosing all the fossil localities where the species was present, and then creating a buffer around the polygon with a radius equal to 10% of the maximum distance between actual fossil occurrences. To account for potential sampling biases, pseudoabsences were geographically placed according to the density of the occurrence data, so that there are more pseudoabsences where presences are denser (Phillips and Dudík 2008, Syfert et al. 2013, Dufresne et al. 2019). Such an approach prevents placing pseudo-absences in regions where no fossil record occurred through time, likely identifying areas where fossilization potential was low (Fourcade et al. 2018, Guevara et al. 2018, Title and Bemmels 2018). We divided the record of each species into 1000-years long consecutive time bins (between the oldest and the youngest occurrence age for the species) and partitioned the 10 000 pseudoabsences proportionally to the number of presences per time bin. For each bin, we then extracted climate data at each occurrence and pseudoabsence point, calibrating a single SDM for each species by pooling occurrence data across temporal bins. SDMs were trained using the maximum entropy modelling algorithm implemented in MAXENT ver. 3.3.3k ('dismo' R package; Phillips et al. 2006). We tested different MAXENT implementations through the 'ENMeval' R package, to find the settings that best optimize the trade-off between goodness-of-fit and overfitting (Muscarella et al. 2014). We tested regularization values between 0.5 and 4, with 0.5 steps. Furthermore, for each of the 100 replicates we tested for the following alternative combinations of feature classes in turn: linear, linear + quadratic, hinge, linear + quadratic + hinge, linear + quadratic + hinge + product and linear + quadratic + hinge + product + threshold (Muscarella et al. 2014). Among the resulting 48 combinations, we chose the model reporting the lowest Akaike information criterion corrected for a small sample size (AICc; Warren and Seifert 2011). The selected model was then evaluated using a temporal block cross-validation approach, splitting the data into 10 temporal bins of approximately equal length, each in turn held out from calibration and used to assess its predictive performance. Block cross-validation approaches proved able to assess model transferability, that is, the ability to extrapolate predictions into new areas/times (Roberts et al. 2017) and to penalize models based on biologically meaningless predictors (Fourcade et al. 2018). Predictive performance was evaluated by calculating the area under the receiver operating characteristic curve (AUC; Swets 1988) and the Boyce index (Hirzel et al. 2006). We dropped SDMs yielding AUC values < 0.7. Finally, for each species, SDMs were projected between the time intervals including, respectively, the species' oldest and youngest occurrence in the fossil record. SDM projections were binarized into presence/absence maps according to three threshold schemes (i.e. 'equalize sensitivity and specificity,' 'maximize TSS,' and '10th percentile of predicted probability'; Liu et al. 2005), to obtain three alternative binary maps for each replicate and time bin. This approach allowed us to include in the subsequent analyses the effect of using different binarization schemes when producing presence/absence maps (below). All the three thresholds were computed by means of the 'PresenceAbsence' R package (Freeman and Moisen 2008).

For each replicate and time bin projection, we calculated a multivariate environmental similarity surface (MESS) to identify the extrapolation areas where climate conditions are non-analogue to conditions considered in model calibration (Fitzpatrick and Hargrove 2009, Elith et al. 2011) and excluded from the binary maps all the suitable cells occurring outside the calibrated predictor space (i.e. showing negative MESS values).

We quantified the effect of age (and associated climatic) uncertainty on predicted distributions by assessing the consensus among the binary maps from the 100 replicates produced for a given species/threshold/time interval. Specifically, we applied the committee averaging method (Thuiller et al. 2009; the mean calculated among the binary maps) over the 100 binarized maps for a given species/threshold/time interval. We calculated the percentage of pixels (geographic cells) reporting a value greater than 0.1 and lower than 0.9 (the uncertainty range). Cells outside the 0.1–0.9 range are taken to represent consistent indication of species presence/absence across the replicates. Cells lower than 0.1 refer to pixels where the 100 replicated SDMs have a consensus in predicting species absence higher than 90%. Cells higher than 0.9 indicate the 100 replicated SDMs have a consensus in predicting species presence higher than 90%. This calculation was replicated for each species/threshold/time interval, except those

SDM replicates achieving an AUC < 0.7 (as done in the main analytical framework), then averaging the results along the time interval axis.

Landscape temporal dynamics

Geographic areas represented by contiguous presence data (cells scored as '1') and entirely surrounded by absence cells (i.e. scored as '0') represent a habitat patch. To retrieve information about aggregation, shape and subdivision of patches, as well as to evaluate their degree of fragmentation in each time bin, we calculated the following six landscape metrics using the 'landscapemetrics' R package (Hesselbarth et al. 2019): total patch area, number of patches, mean patch area, mean Euclidean nearest-neighbour distance, aggregation index and division index. The number of patches represents a simple measure of the fragmentation extent, while the mean patch area gives information about how the habitat patches of a particular landscape are growing or merging over time (McGarigal et al. 2012). Division index yields the probability that two randomly selected cells are not located in the same patch. Mean Euclidean nearest-neighbour distance accounts for the number of highly isolated patches, whereas aggregation index evaluates the frequency with which patch pairs occur side-by-side in the landscape (McGarigal et al. 2012, Zatelli et al. 2019). We selected these metrics as they can be successfully used to compare fragmentation among different landscapes and, in our case, different time bins (He et al. 2000, Cornejo-Denman et al. 2020). These metrics were calculated for each species in each 1 ka time bin (limited to the temporal range of the species fossils), each replicated date and binarization threshold, combining all the results in a single dataset. The outcomes were used to describe the temporal dynamics of habitat patch configuration during the last 200 ka by fitting linear mixed models (LMMs), where each of the landscape metrics was used as the response variable and the time (in kilo years, from 200 to 2 ka), as the explanatory variable. Response variables were first transformed using a logarithmic transformation to improve normality. In addition, since we were interested in testing for different temporal dynamics of spatial patch configuration for extinct and extant species, LMMs were fitted putting the 'time' explanatory variable in interaction with the species status (i.e. extinct or extant). This setup allowed LMMs to fit two different landscape metric-versus-time relationships for extinct and extant species.

As we did not have an a priori expectation about the shape of the relationship between landscape metrics and time, we accounted for possible non-linear patterns by fitting LMMs with linear, linear + quadratic and linear + quadratic + cubic relationships. To avoid overly complex or overfitted models, LMMs including quadratic and cubic terms were compared with linear terms using AIC. To account for differences in metric values among the different species, replicated datasets and binarization thresholds, we included such factors as random effects in LMMs, allowing the models to vary their intercepts accordingly. Models' goodness-of-fit was assessed by calculating the conditional coefficient of determination for LMM (R^2; Nakagawa and Schielzeth 2013). Furthermore, we evaluated the LMMs' predictive accuracy by calculating Pearson's correlation coefficient between observed and predicted values of the outcome under a five-fold cross-validation scheme. All the statistical analyses were run by using the 'lme4', 'MuMIn' and 'performance' R packages.

To assess the relative contribution of the landscape metrics and functional traits (body mass and diet, Koch and Barnosky 2006, Galetti et al. 2017) in discriminating between extinct and extant species, we ran a Random Forest classification model (RF; Breiman 2001) using the 'caret' R package (Kuhn 2018). In this model, we used the status of each species ('extinct' versus 'extant') as the response variable, while the landscape metrics, body mass, diet, time in kilo-years, replicated datasets and binarization thresholds were included as explanatory variables. Before entering the RF model, the six landscape metrics were checked for multicollinearity (i.e. VIF ≤ 5; Zuur et al. 2010), retaining aggregation index, mean patch area, mean Euclidean nearest-neighbor distance, number of patches and division index. We evaluated the RF model's ability to correctly classify a species as extinct or extant according to the abovementioned covariates by calculating the AUC under a five-fold cross-validation scheme. In particular, we optimally tuned RF settings by testing for different combinations of the number of variables randomly selected at each node, depth of the classification trees created by the algorithm and splitting rule parameters (Gini index and ExtraTrees algorithm). All RF candidate models were run allowing a maximum of 1000 trees. Once optimally tuned, the RF model was used to quantify the relative importance of each covariate, expressed as the mean decrease accuracy (i.e. how much accuracy the model loses by excluding each variable in turn, Kuhn 2018). We cumulated the mean decrease in accuracy across variables in four macro-categories: landscape metrics, diet, mass and other effects (i.e. time in kilo-years, replicated datasets and binarization thresholds). In addition, we generated partial dependence plots according to Greenwell (2017), to depict the shape of the relationship between each explanatory variable and the probability of a given species being classified as 'extinct' while holding the values of other variables constant.

Results

Among the species considered, 22 had at least one SDM with AUC > 0.7 (Supporting information for more details). Overall, SDMs for these 22 species reached fair predictive performances (sensu Swets 1988), with *Megaloceros giganteus* reporting the lowest AUC values (0.702, SD = 0.002), and *Equus hydruntinus* showing the highest (0.796, SD = 0.017; Supporting information). As for Boyce index, *Lynx pardinus* achieved the lowest values (0.438, SD = 0.138), while *Cervus elaphus* reported the highest (0.894, SD = 0.015; Supporting information). The percentage of geographic cells within the

uncertainty range averaged over all species was some 8%, indicating the effect of age uncertainty on SDMs to be rather marginal (Supporting information).

For all landscape metrics, LMMs including linear, quadratic and cubic relationships had the lowest AICc. Such models achieved a high goodness-of-fit, with conditional R^2 values ranging between 0.369 for mean Euclidean nearest-neighbour distance to 0.828 for total patch area (Table 1). Predictive accuracy was high for all the LMMs, with correlation values between 0.539 (SD = 0.004) for mean Euclidean nearest-neighbour distance and 0.889 (SD = 0.001) for total patch area (Table 1).

Aggregation index, mean patch area and total patch area exhibited similar patterns in their temporal dynamics, though reporting different magnitudes between extinct and extant species. For extinct species, there was a substantial decline in the value of these three metrics between 200 and 150 ka (Fig. 1), followed by a turning point and significant upward concavity (significant cubic term; Table 2) that led to subsequent increasing trends centered around 70 ka (Fig. 1). After that time, the curves for these three metrics showed another turning point with a significant downward concavity (significant quadratic term, Table 2, Fig. 1), significantly decreasing towards the present time (significant linear terms; Table 2). Temporal dynamics of mean patch area and total patch area for extant species showed opposite shapes compared to extinct species (Fig. 1, Table 2). Aggregation index showed rather constant temporal dynamics for extant species, reporting a single downward concavity around 120 ka (quadratic term is significant, while cubic term is not; Table 2).

Number of patches for extinct species steeply increased between 200 and 100 ka (Fig. 1), when it exhibits a single downward concavity (quadratic term is significant, while cubic term is not; Table 2), followed by a monotonic decrease (significant linear term; Table 2). The number of patches for extant species showed less pronounced temporal fluctuations than extinct ones, reporting a slight upward concavity around 180 ka, a significant downward concavity around 80 ka (significant quadratic coefficient; Table 2) and a subsequent moderate decline towards the present (significant linear term; Table 2, Fig. 1). Mean Euclidean nearest-neighbour distance and division index shared similar temporal trends. For the extinct group, both these metrics showed a steep decrease up to ca 120 and 80 ka, respectively, where they reach significant tipping points and upward concavities (significant quadratic coefficients; Table 2). Subsequently, the two metrics increase again (linear terms are significant; Table 2), though this final trend is more pronounced in the division index (Fig. 1). As for extant species, mean Euclidean nearest-neighbour distance and division index showed very similar patterns, with a first upward concavity around 150 ka (Table 2, Fig. 1), a second downward concavity around 50 ka (Table 2, Fig. 1) and a final decrease towards the present (Table 2, Fig. 1).

We used the LMM equations to calculate the last intersection points between extinct and extant polynomials. Calculating this point is useful to understand when, in time, the paths of landscape metrics diverged between extant and extinct mammals. We found that mean and total patch area, division index and mean patch distance took different directions in extant as compared to extinct species during the 40–30 ka time span. Division index and mean patch distance increased in extinct species from that moment towards the present, whereas the opposite took place for extant taxa. The number of patches and aggregation index started to decrease at roughly the same time for all species, yet the decrease was much steeper for extinct species.

The RF model achieved an excellent ability to discriminate between extant and extinct species (AUC = 0.998; Supporting information). Ranking of variable importance showed a predominant role of body mass (mean decrease accuracy = 38.91%), followed by landscape metrics, which contributed to 37.77% collectively, diet (19.53%) and then

Table 1. Results of AIC analysis for three competing models. Table reports AIC, conditional R^2 and accuracy (with associated standard deviation) values. The models are estimated for each landscape metric separately.

Metric	Relationship	AIC	Conditional R^2	Accuracy
Aggregation index	Linear	−815 511.0642	0.7064	0.7806 (0.004)
	Linear + quadratic	−816 352.5136	0.7071	0.7812 (0.005)
	Linear + quadratic + cubic	−817 311.1986	0.7078	0.7821 (0.002)
Mean patch area	Linear	302 423.3057	0.7415	0.8094 (0.003)
	Linear + quadratic	301 276.0860	0.7420	0.8102 (0.003)
	Linear + quadratic + cubic	300 280.2434	0.7426	0.8109 (0.003)
Total patch area	Linear	305 014.2171	0.8255	0.8878 (0.003)
	Linear + quadratic	300 889.6698	0.8286	0.8894 (0.001)
	Linear + quadratic + cubic	300 091.3539	0.8289	0.8897 (0.001)
Mean patch distance	Linear	−130 544.8501	0.3679	0.5382 (0.007)
	Linear + quadratic	−130 949.5449	0.3697	0.5391 (0.005)
	Linear + quadratic + cubic	−131 302.4571	0.3699	0.5399 (0.004)
Number of patches	Linear	72 200.3817	0.6941	0.8088 (0.004)
	Linear + quadratic	70 173.0404	0.6984	0.8102 (0.003)
	Linear + quadratic + cubic	70 134.0096	0.6987	0.8102 (0.003)
Division index	Linear	175 984.8104	0.5241	0.6803 (0.007)
	Linear + quadratic	174 614.6971	0.5223	0.6820 (0.003)
	Linear + quadratic + cubic	174 214.7835	0.5232	0.6825 (0.006)

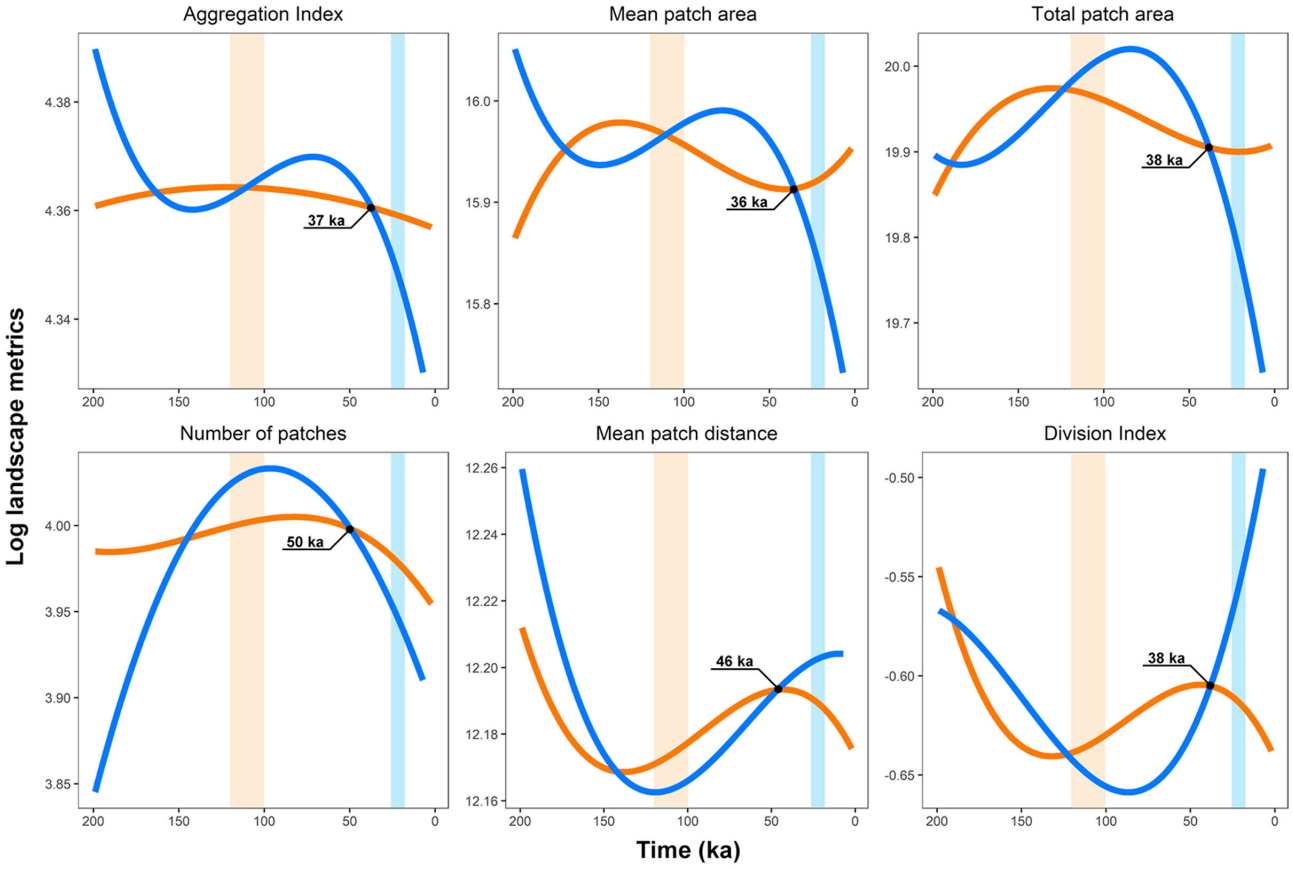

Figure 1. The relationship between landscape metrics (logged values) and time fitted by LMMs, plotted for extinct (blue line) and extant species (orange line). The vertical orange band highlights the Eemian period (120–100 ka), while light blue band highlights the Last Glacial Maximum period (26–18 ka).

additional effects (2.60%). Partial dependence plots showed the probability of being classified as 'extinct' to decrease towards higher values of aggregation index and mean patch area (Fig. 2). Moreover, extinction probability increases towards higher values of mean patch distance, number of patches, division index and body mass (Fig. 2). As for diet, the probability of being classified as 'extinct' is higher for species exhibiting a more specialized diet (i.e. strict grazers, browsers or carnivores; Fig. 2).

Discussion

The imprint of humans on wildlife has gone through a long history, tracing back to the Late Pleistocene, when *Homo sapiens* started to colonize the world biota outside its African homeland, contributing to a massive extinction crisis affecting large mammals worldwide (Rule et al. 2012, Sandom et al. 2014, Berti and Svenning 2020). The effect of *H. sapiens* on its mammalian preys and competitors is more apparent where species were naïve to the new super-predator, that is in the Americas and Oceania, whilst the signature of human effects is milder in Africa and Eurasia (where megafauna species and *H. sapiens* had been in contact much longer) and possibly superseded by the contemporary effects of intense global climate change there (Cooper et al. 2015, Carotenuto et al. 2016, Di Febbraro et al. 2017). Current, large-scale investigations on Pleistocene ecosystems and their evolution are common for North America (Tóth et al. 2019, Seersholm et al. 2020) and Oceania (Rule et al. 2012, Hocknull et al. 2020) but rare for Eurasia, despite the high-quality fossil record. Eurasia thus offers the unique opportunity to test the effect of geographic habitat structure on species survival. Here we grasp this opportunity by using SDMs to model habitat patches size, number and isolation overtime for 22 large mammal species, including both extinct and extant taxa. This modelling effort indicates that extinct mammals went through considerable deterioration of habitat geographic structure during the last glacial period and started to fare worse than extant species from about 50 ka (Fig. 3, Supporting information). Late Pleistocene Eurasian large mammals had their best survival conditions when several well-connected habitat patches were available, which allowed maintenance of healthy metapopulation structures (Hanski and Mononen 2011, Englund et al. 2020). For now-extinct species, the degree of connection among patches started to deteriorate noticeably during the 46–36 ka interval (Fig. 1–3, Supporting information). Although this figure is derived

Table 2. Summary of statistics for the optimal linear mixed models as indicated by the Akaike information criterion. For each model, slope ('Estimate'), standard error ('SE') and p-value referred to both extinct and extant group are reported.

Metric	Status	Estimate	SE	p-value
Aggregation index	intercept	4.363	0.042	<0.001
	poly(time, 3)1	0.811	0.085	<0.001
	poly(time, 3)2	−0.683	0.079	<0.001
	poly(time, 3)3	−0.027	0.079	0.737
	poly(time, 3)1:statusextint	2.413	0.113	<0.001
	poly(time, 3)2:statusextint	−2.223	0.118	<0.001
	poly(time, 3)3:statusextint	3.694	0.119	<0.001
Mean patch area	intercept	15.945	0.311	<0.001
	poly(time, 3)1	8.604	0.548	<0.001
	poly(time, 3)2	−4.165	0.509	<0.001
	poly(time, 3)3	−9.689	0.510	<0.001
	poly(time, 3)1:statusextint	16.826	0.730	<0.001
	poly(time, 3)2:statusextint	−19.025	0.757	<0.001
	poly(time, 3)3:statusextint	19.308	0.764	<0.001
Total parch area	intercept	19.939	0.385	<0.001
	poly(time, 3)1	10.029	0.548	<0.001
	poly(time, 3)2	−9.216	0.509	<0.001
	poly(time, 3)3	−7.484	0.510	<0.001
	poly(time, 3)1:statusextint	18.771	0.730	<0.001
	poly(time, 3)2:statusextint	−40.518	0.757	<0.001
	poly(time, 3)3:statusextint	18.494	0.764	<0.001
Mean patch distance	intercept	12.183	0.061	<0.001
	poly(time, 3)1	−3.028	0.267	<0.001
	poly(time, 3)2	1.315	0.248	<0.001
	poly(time, 3)3	3.791	0.248	<0.001
	poly(time, 3)1:statusextint	−3.237	0.356	<0.001
	poly(time, 3)2:statusextint	7.836	0.369	<0.001
	poly(time, 3)3:statusextint	4.165	0.372	<0.001
Number of patches	intercept	3.993	0.107	<0.001
	poly(time, 3)1	1.421	0.373	<0.001
	poly(time, 3)2	−5.050	0.347	<0.001
	poly(time, 3)3	2.206	0.347	<0.001
	poly(time, 3)1:statusextint	1.946	0.497	<0.001
	poly(time, 3)2:statusextint	−21.494	0.516	<0.001
	poly(time, 3)3:statusextint	−0.813	0.521	0.118
Division index	intercept	−0.622	0.150	0.035
	poly(time, 3)1	−2.691	0.444	<0.001
	poly(time, 3)2	3.448	0.413	<0.001
	poly(time, 3)3	7.151	0.413	<0.001
	poly(time, 3)1:statusextint	−6.780	0.592	<0.001
	poly(time, 3)2:statusextint	19.673	0.614	<0.001
	poly(time, 3)3:statusextint	−6.305	0.619	<0.001

from modelling based on inferred climatic preferences and must therefore be interpreted with caution, it is intriguing to note how this period of time nicely coincides with moments of megafauna extinction or strong population decline. In fact, the best radiometric estimates for the extinction date of *Homo neanderthalensis* (at 40 ka, Higham et al. 2014) the giant rhino *Elasmotherium sibiricum* (Kosintsev et al. 2019) the camel *Camelus knoblochi*, the giant deer *Sinomegaceros yabei*, the narrow-nosed rhino *Stephanorhinus hemitoechus*, the antelope *Spiroceros kiakhtensis* and the Asian straight-tusked elephant *Palaeoloxodon naumanni* are all concentrated in the narrow 45–37 ka interval (Stuart and Lister 2012). Mitochondrial DNA and population demographics suggest the cave bear *Ursus spelaeus* suffered a dramatic population decline starting at 50 ka (Mondanaro et al. 2019). The same rapid decline in exactly the same time interval pertains to the Eurasian populations of cave lion *Panthera leo spelaea* (Stuart and Lister 2011), and cave hyena *Crocuta crocuta spelaea* (Stuart and Lister 2014). Our modelling results indicate that mean patch area and total area for the extinct species dwindle later than the number of patches and their degree of aggregation, and that the average distance between patches differs the most between extinct and extant species. These results indicate that extinct species begun their path to extinction by losing occupied territories and splitting into increasingly more isolated patches almost in coincidence to human arrival in Eurasia (Hublin et al. 2020, Weber et al. 2020). Albeit our data do not allow testing whether modern humans or

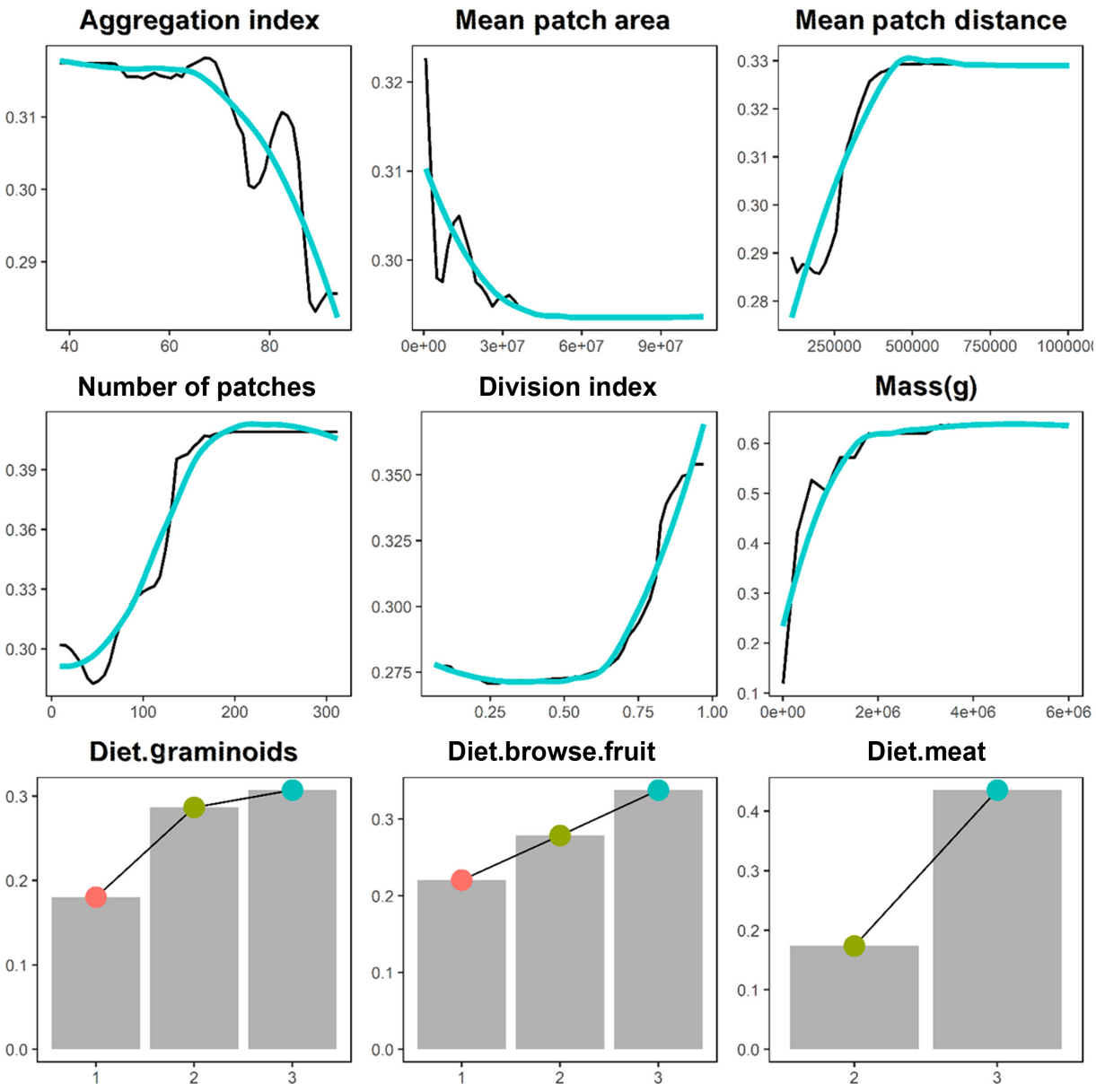

Figure 2. Partial dependency plots derived from RF model. On the y axis (not to the same scale) the probability to be classified as 'extinct'. Smoothed response curves are represented in cyan. The coloured points depicted in the third row represent the different rank of diet category.

climate change were the most important cause of increased habitat fragmentation for the extinct species, the fossil record suggests that the extinction wave must have initiated at northern latitudes. Most extinct megafauna persisted in the Mediterranean area, and in the far East, before extinction, abandoning northernmost habitats first (e.g. cave hyaena, Stuart and Lister 2014; cave lion, Stuart and Lister 2011; cave bear, Mondanaro et al. 2019; Neanderthals, Fabre et al. 2009). In fact, the presence of glacial refugia and cryptic northern refugia may have only increased habitat patchiness for the Eurasian megafauna as a whole (Hewitt 2000, Bhagwat and Willis 2008) and testifies to this progressive retreat from the north. Extant species instead resisted this retraction or else showed similar retraction patterns but were able to survive the glacial period, and their landscape metrics all indicated a higher degree of habitat connectivity after the last glacial maximum.

The importance of habitat fragmentation to species survival is confirmed by the random forest models. Landscape metrics collectively explain 38% of the probability to classify a species as extinct or extant, a notable figure considering that the corresponding figure for body mass, which is the single best-known factor characterizing the megafauna extinction is just 3–4 times higher than individual landscape metric. Among individual landscape metrics, changes in the number of patches and their division index increased the chance of

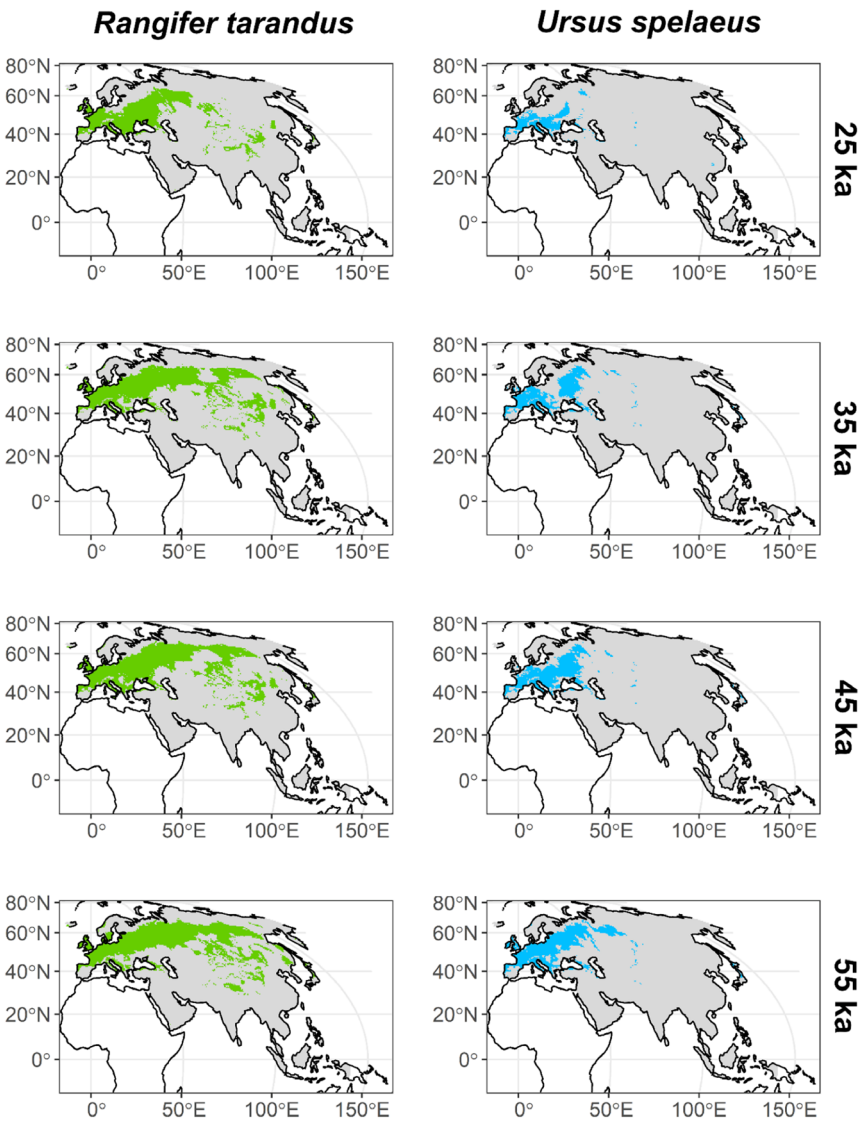

Figure 3. Habitat suitability maps for *Rangifer tarandus* and *Ursus spelaeus* over four consecutive time intervals. The R codes to reproduce these figures for all species over all time intervals are available as Supporting information.

extinction by as much as 10% each, pointing to a pervasive effect of the degree of fragmentation on species survival. Total patch area was collinear to mean patch area and therefore excluded from the model. Yet, the importance of mean patch area to the likelihood of classifying a species as extinct is half as important as the number of patches and division index. This suggests that fragmentation is more important to survival than the total amount of habitat.

The classification of species into dietary categories suggests that the feeding habits had some influence on megafauna extinction. We do not have sufficient data on carnivores to trust the results for these species, yet for herbivores, grazing species were more affected than those feeding on browse or mixed diet. This correlates well to the notion that by the end of the Pleistocene the so-called mammoth steppe, a widespread habitat extending from central Europe to the Kamchatka started to vanish together with its habitat specialists, such as the mammoth or the woolly rhino (Zimov et al. 2012, Yeakel et al. 2013). Browse specialists, like the straight-tusked elephant and hippopotamus, were similarly affected by the disappearance of forested areas around 70 ka, which might have been responsible for their extinction at that time and might explain the apparent trend for increasing extinction risk with an increased amount of browse in the diet (Fig. 2).

There is strong evidence that fragmentation increases extinction risk in individual species (Safi and Kerth 2004, Wang et al. 2014, Lino et al. 2019). Our study does not contradict the habitat amount hypothesis (HAH), posing that the total available habitat size matters more than its fragmentation to species diversity. Yet, our data strongly suggest that on a long temporal scale, the positive metapopulation feedback and the possibility to survive via habitat tracking reaching refugia matters more to biodiversity than habitat size per se.

Climate change is one of the main forces that will exert its effects on biodiversity in the coming years (Warren et al. 2018), and we highlight its role in determining habitat fragmentation in the last 200 ka. Our results show that patterns of habitat fragmentation through time differ considerably between extinct and extant Eurasian megafauna, unveiling a possible pathway of rapid species decline at ca 50 ka. Species can adapt to some level of climate change through dispersal, phenotypic plasticity and evolutionary adaptation (Diniz-Filho et al. 2019), but most species risk facing shrinkage in their niche under high levels of change (Di Marco et al. 2021). The current velocity of climate change (Loarie et al. 2009) means megafauna in other continents (such as Africa) might face similar risk to that faced by Eurasian species in the Late Pleistocene, and even remaining species in Eurasia might be at risk. The scale of the problem means that achieving bold climate mitigation targets, such as those established under the Paris agreement, is paramount to reducing the risk of losing some of the most iconic mammals that have survived to the present day. Even so, active conservation interventions, such as habitat restoration, the creation of habitat corridors and species translocation, will likely be necessary for some species.

Acknowledgements – We are grateful to Brandon Greenwell for his help with pdp functions usage. Yue Wang, and an anonymous reviewer provided us with important advice on an earlier version of the manuscript.
Funding – Moreno Di Marco was supported by MIUR Rita Levi Montalcini programme.
Conflicts of interest – The authors declare no competing interest.

Author contributions

Alessandro Mondanaro: Conceptualization (equal); Data curation (lead); Formal analysis (lead); Funding acquisition (equal); Writing – original draft (equal). **Mirko Di Febbraro**: Conceptualization (equal); Data curation (equal); Formal analysis (lead); Writing – original draft (equal). **Marina Melchionna**: Data curation (equal); Visualization (equal); Writing – original draft (equal); Writing – review and editing (equal). **Luigi Maiorano**: Methodology (equal); Writing – original draft (equal); Writing – review and editing (equal). **Moreno Di Marco**: Methodology (equal); Writing – original draft (equal); Writing – review and editing (equal). **Neil Edwards**: Methodology (equal); Resources (equal); Writing – original draft (equal); Writing – review and editing (equal). **Philip Holden**: Methodology (equal); Resources (equal); Writing – original draft (equal); Writing – review and editing (equal). **Silvia Castiglione**: Visualization (equal); Writing – original draft (equal); Writing – review and editing (equal). **Lorenzo Rook**: Funding acquisition (equal); Writing – original draft (equal); Writing – review and editing (equal). **Pasquale Raia**: Conceptualization (equal); Writing – original draft (lead); Writing – review and editing (equal).

Transparent Peer Review

The peer review history for this article is available at <https://publons.com/publon/10.1111/ecog.05939>.

Data availability statement

Data are available from the Dryad Digital Repositor: <http://dx.doi.org/10.5061/dryad.4xgxd259k> (Mondanaro et al. 2021).

References

Andermann, T. et al. 2020. The past and future human impact on mammalian diversity. – Sci. Adv. 6: eabb2313.
Berger, A. and Loutre, M.-F. 1999. Parameters of the Earth's orbit for the last 5 Million years in 1 kyr resolution. – PANGAEA
Berti, E. and Svenning, J.-C. 2020. Megafauna extinctions have reduced biotic connectivity worldwide. – Global Ecol. Biogeogr. 29: 2131–2142.
Bhagwat, S. A. and Willis, K. J. 2008. Species persistence in northerly glacial refugia of Europe: a matter of chance or biogeographical traits? – J. Biogeogr. 35: 464–482.
Blomqvist, D. et al. 2010. Trapped in the extinction vortex? Strong genetic effects in a declining vertebrate population. – BMC Evol. Biol. 10: 1–9.
Breiman, L. 2001. Random forests. – Mach. Learn. 45: 5–32.
Carotenuto, F. et al. 2016. The influence of climate on species distribution over time and space during the late Quaternary. – Quat. Sci. Rev. 149: 188–199.
Ceballos, G. et al. 2015. Accelerated modern human-induced species losses: entering the sixth mass extinction. – Sci. Adv. 1: e1400253.
Cooper, A. et al. 2015. Abrupt warming events drove Late Pleistocene Holarctic megafaunal turnover. – Science 349: 602–606.
Cornejo-Denman, L. et al. 2020. Landscape dynamics in an iconic watershed of northwestern Mexico: vegetation condition insights using landsat and PlanetScope data. – Remote Sens. 12: 2519.
Di Febbraro, M. et al. 2017. Does the jack of all trades fare best? Survival and niche width in Late Pleistocene megafauna. – J. Biogeogr. 44: 2828–2838.
Di Marco, M. et al. 2021. Drivers of change in the realised climatic niche of terrestrial mammals. – Ecography 44: 1180–1190.
Diamond, J. M. 1975. The island dilemma: lessons of modern biogeographic studies for the design of natural reserves. – Biol. Conserv. 7: 129–146.
Diniz-Filho, J. A. F. et al. 2019. A macroecological approach to evolutionary rescue and adaptation to climate change. – Ecography 42: 1124–1141.
Dufresne, E. R. et al. 2019. Modeling the distribution of a wide-ranging invasive species using the sampling efforts of expert and citizen scientists. – Ecol. Evol. 9: 11053–11063.
Elith, J. et al. 2011. A statistical explanation of MaxEnt for ecologists. – Divers. Distrib. 17: 43–57.
Englund, G. et al. 2020. Holocene extinctions of a top predator – effects of time, habitat area and habitat subdivision. – J. Anim. Ecol. 89: 1202–1215.
Fabre, V. et al. 2009. Genetic evidence of geographical groups among neanderthals. – PLoS One 4: e5151.

Fahrig, L. 2003. Effects of habitat fragmentation on biodiversity. – Annu. Rev. Ecol. Evol. 34: 487–515.
Fahrig, L. 2013. Rethinking patch size and isolation effects: the habitat amount hypothesis. – J. Biogeogr. 40: 1649–1663.
Fahrig, L. 2020. Why do several small patches hold more species than few large patches? – Global Ecol. Biogeogr. 29: 615–628.
Fahrig, L. et al. 2019. Is habitat fragmentation bad for biodiversity? – Biol. Conserv. 230: 179–186.
Fitzpatrick, M. C. and Hargrove, W. W. 2009. The projection of species distribution models and the problem of non-analog climate. – Biodivers. Conserv. 18: 2255–2261.
Fourcade, Y. et al. 2018. Paintings predict the distribution of species, or the challenge of selecting environmental predictors and evaluation statistics. – Global Ecol. Biogeogr. 27: 245–256.
Freeman, E. A. and Moisen, G. 2008. PresenceAbsence: an R package for presence absence analysis. – J. Stat. Softw. 23: 31.
Galetti, M. et al. 2017. Ecological and evolutionary legacy of megafauna extinctions. – Biol. Rev. 292: 1893–1899.
Greenwell, B. M. 2017. pdp: an R package for constructing partial dependence plots. – R J. 9: 421.
Guevara, L. et al. 2018. Toward ecologically realistic predictions of species distributions: a cross-time example from tropical montane cloud forests. – Global Change Biol. 24: 1511–1522.
Haddad, N. M. et al. 2015. Habitat fragmentation and its lasting impact on Earth's ecosystems. – Sci. Adv. 1: e1500052.
Hanski, I. and Mononen, T. 2011. Eco-evolutionary dynamics of dispersal in spatially heterogeneous environments. – Ecol. Lett. 14: 1025–1034.
He, H. S. et al. 2000. An aggregation index (AI) to quantify spatial patterns of landscapes. – Landscape Ecol. 15: 591–601.
Hesselbarth, M. H. K. et al. 2019. landscapemetrics: an open-source R tool to calculate landscape metrics. – Ecography 42: 1648–1657.
Hewitt, G. 2000. The genetic legacy of the Quaternary ice ages. – Nature 405: 907–913.
Higham, T. et al. 2014. The timing and spatiotemporal patterning of Neanderthal disappearance. – Nature 512: 306–309.
Hirzel, A. H. et al. 2006. Evaluating the ability of habitat suitability models to predict species presences. – Ecol. Model. 199: 142–152.
Hocknull, S. A. et al. 2020. Extinction of eastern Sahul megafauna coincides with sustained environmental deterioration. – Nat. Commun. 11: 1–14.
Holden, P. B. et al. 2016. PLASIM-GENIE v1.0: a new intermediate complexity AOGCM. – Geosci. Model Dev. 9: 3347–3361.
Holden, P. B. et al. 2019. PALEO-PGEM v1.0: a statistical emulator of Pliocene–Pleistocene climate. – Geosci. Model Dev. 12: 5137–5155.
Hublin, J.-J. et al. 2020. Initial upper palaeolithic homo sapiens from Bacho Kiro Cave, Bulgaria. – Nature 581: 299–302.
Karger, D. N. et al. 2017. Climatologies at high resolution for the earth's land surface areas. – Sci. Data 4: 170122.
Koch, P. L. and Barnosky, A. D. 2006. Late quaternary extinctions: state of the debate. – Annu. Rev. Ecol. Evol. Syst. 37: 215–250.
Kosintsev, P. et al. 2019. Evolution and extinction of the giant rhinoceros *Elasmotherium sibiricum* sheds light on late Quaternary megafaunal extinctions. – Nat. Ecol. Evol. 3: 31–38.
Kuhn, M. et al. 2018. caret: classification and regression training (R package). R package ver., 6-0. – <https://CRAN.R-project.org/package=caret>.
Lino, A. et al. 2019. A meta-analysis of the effects of habitat loss and fragmentation on genetic diversity in mammals. – Mamm. Biol. 94: 69–76.
Liu, C. et al. 2005. Selecting thresholds of occurrence in the prediction of species distributions. – Ecography 28: 385–393.
Liu, X. et al. 2019. Global urban expansion offsets climate-driven increases in terrestrial net primary productivity. – Nat. Commun. 10: 5558.
Loarie, S. R. et al. 2009. The velocity of climate change. – Nature 462: 1052–1055.
Lundgren, E. J. et al. 2021. Functional traits of the world's late Quaternary large-bodied avian and mammalian herbivores. – Sci. Data: 1–21.
Lüthi, D. et al. 2008. High-resolution carbon dioxide concentration record 650 000–800 000 years before present. – Nature 453: 379–382.
Lyons, S. K. et al. 2016. Holocene shifts in the assembly of plant and animal communities implicate human impacts. – Nature 529: 80–83.
McGarigal, K. et al. 2012. FRAGSTATS v4: spatial pattern analysis program for categorical and continuous maps. – Computer software program produced by the authors at the Univ. of Massachusetts, Amherst.
Mondanaro, A. et al. 2019. Additive effects of climate change and human hunting explain population decline and extinction in cave bears. – Boreas 48: 605–615.
Mondanaro, A. et al. 2021. Data from: The role of habitat fragmentation in Pleistocene megafauna extinction in Eurasia. – Dryad Digital Repository, <http://dx.doi.org/10.5061/dryad.4xgxd259k>.
Muscarella, R. et al. 2014. ENMeval: an R package for conducting spatially independent evaluations and estimating optimal model complexity for Maxent ecological niche models. – Methods Ecol. Evol. 5: 1198–1205.
Naimi, B. et al. 2014. Where is positional uncertainty a problem for species distribution modelling? – Ecography 37: 191–203.
Nakagawa, S. and Schielzeth, H. 2013. A general and simple method for obtaining R2 from generalized linear mixed-effects models. – Methods Ecol. Evol. 4: 133–142.
Newbold, T. et al. 2015. Global effects of land use on local terrestrial biodiversity. – Nature 520: 45–50.
Parnell, A. 2016. Bchron: radiocarbon dating, age-depth modelling, relative sea level rate estimation and non-parametric phase modelling. R package ver. 4.1.1. – <https://andrewcparnell.github.io/Bchron/>
Phillips, S. J. and Dudík, M. 2008. Modeling of species distributions with Maxent: new extensions and a comprehensive evaluation. – Ecography 31: 161–175.
Phillips, S. J. et al. 2006. Maximum entropy modeling of species geographic distributions. – Ecol. Model. 190: 231–259.
Pimiento, C. et al. 2020. Functional diversity of marine megafauna in the Anthropocene. – Sci. Adv. 6: eaay7650.
Raia, P. et al. 2009. More than three million years of community evolution. The temporal and geographical resolution of the Plio-Pleistocene western Eurasia mammal faunas. – Palaeogeogr. Palaeoclimatol. Palaeoecol. 276: 15–23.
Raia, P. et al. 2020. Past extinctions of homo species coincided with increased vulnerability to climatic change. – One Earth 3: 480–490.
Reed, D. H. 2004. Extinction risk in fragmented habitats. – Anim. Conserv. 7: 181–191.
Reimer, P. J. et al. 2020. The IntCal20 Northern Hemisphere radiocarbon age calibration curve (0–55 cal kBP). – Radiocarbon 62: 725–757.
Ripple, W. J. et al. 2019. Are we eating the world's megafauna to extinction? – Conserv. Lett. 12: e12627.

Roberts, D. R. et al. 2017. Cross-validation strategies for data with temporal, spatial, hierarchical or phylogenetic structure. – Ecography 40: 913–929.
Rule, S. et al. 2012. The aftermath of megafaunal extinction: ecosystem transformation in Pleistocene Australia. – Science 335: 1483–1486.
Safi, K. and Kerth, G. 2004. A comparative analysis of specialization and extinction risk in temperate-zone bats. – Conserv. Biol. 18: 1293–1303.
Sandom, C. et al. 2014. Global late Quaternary megafauna extinctions linked to humans, not climate change. – Proc. Biol. Sci. 281: 20133254.
Saura, S. 2021. The habitat amount hypothesis implies negative effects of habitat fragmentation on species richness. – J. Biogeogr. 48: 11–22.
Seersholm, F. V. et al. 2020. Rapid range shifts and megafaunal extinctions associated with late Pleistocene climate change. – Nat. Commun. 11: 1–10.
Stap, L. B. et al. 2017. The influence of ice sheets on temperature during the past 38 million years inferred from a one-dimensional ice sheet-climate model. – Clim. Past 13: 1243–1257.
Stuart, A. J. and Lister, A. M. 2011. Extinction chronology of the cave lion *Panthera spelaea*. – Quat. Sci. Rev. 30: 2329–2340.
Stuart, A. J. and Lister, A. M. 2012. Extinction chronology of the woolly rhinoceros *Coelodonta antiquitatis* in the context of late Quaternary megafaunal extinctions in northern Eurasia. – Quat. Sci. Rev. 51: 1–17.
Stuart, A. J. and Lister, A. M. 2014. New radiocarbon evidence on the extirpation of the spotted hyaena (*Crocuta crocuta* (Erxl.)) in northern Eurasia. – Quat. Sci. Rev. 96: 108–116.
Swets, J. A. 1988. Measuring the accuracy of diagnostic systems. – Science 240: 1285–1293.
Syfert, M. M. et al. 2013. The effects of sampling bias and model complexity on the predictive performance of MaxEnt species distribution models. – PLoS One 8: e55158.
Thuiller, W. et al. 2009. BIOMOD – a platform for ensemble forecasting of species distributions. – Ecography 32: 369–373.
Title, P. O. and Bemmels, J. B. 2018. ENVIREM: an expanded set of bioclimatic and topographic variables increases flexibility and improves performance of ecological niche modeling. – Ecography 41: 291–307.
Tjørve, E. 2010. How to resolve the SLOSS debate: lessons from species-diversity models. – J. Theor. Biol. 264: 604–612.
Tóth, A. B. et al. 2019. Reorganization of surviving mammal communities after the end-Pleistocene megafaunal extinction. – Science 365: 1305–1308.
Wang, X. et al. 2014. Measuring habitat fragmentation: an evaluation of landscape pattern metrics. – Methods Ecol. Evol. 5: 634–646.
Warren, D. L. and Seifert, S. N. 2011. Ecological niche modeling in Maxent: the importance of model complexity and the performance of model selection criteria. – Ecol. Appl. 21: 335–342.
Warren, R. et al. 2018. The projected effect on insects, vertebrates and plants of limiting global warming to 1.5°C rather than 2°C. – Science 360: 791–795.
Weber, G. W. et al. 2020. Before the massive modern human dispersal into Eurasia: a 55 000-year-old partial cranium from Manot Cave, Israel. – Quat. Int. 551: 29–39.
Williams, B. A. et al. 2020. Change in terrestrial human footprint drives continued loss of intact ecosystems. – One Earth 3: 371–382.
Yeakel, J. D. et al. 2013. The impact of climate change on the structure of Pleistocene food webs across the mammoth steppe. – Proc. R. Soc. B 280: 20130239.
Zatelli, P. et al. 2019. Relevance of the cell neighborhood size in landscape metrics evaluation and free or open source software implementations. – ISPRS Int. J. Geo-Inform. 8: 586.
Zimov, S. A. et al. 2012. Mammoth steppe: a high-productivity phenomenon. – Quat. Sci. Rev. 57: 26–45.
Zuur, A. F. et al. 2010. A protocol for data exploration to avoid common statistical problems. – Methods Ecol. Evol. 1: 3–14.